



# Identification of Species-Preserved Cortical Landmarks

Tuo Zhang<sup>1</sup>(✉), Xiao Li<sup>1</sup>, Lin Zhao<sup>1</sup>, Ying Huang<sup>1</sup>, Lei Guo<sup>1</sup>,  
and Tianming Liu<sup>2</sup>

<sup>1</sup> Brain Decoding Research Center, Northwestern Polytechnical University,  
Xi'an, Shaanxi, China

tuo Zhang@nwpu.edu.cn

<sup>2</sup> Computer Science Department, The University of Georgia, Athens, GA, USA

**Abstract.** Primate brain evolution has been an intriguing research topic for centuries. Previous comparative studies focused on identification of species-preserved cortical landmarks or axonal pathways via approaches such as registration. However, because of huge cross-species variations, these studies dealt with only a few specific fasciculi and cortices or relied on a predefined brain parcellation shared among species. In this work, we used T1-weighted MRI data and diffusion MRI data to identify novel landmarks on entire cortices based on folding patterns on macaque and human brains and further proposed a pipeline to establish cross-species correspondence for them based on networks derived from streamline fibers. Our experimental results are consistent with the reports in the literature, demonstrating the effectiveness and promise of this framework. The merits of this work lie in not only the identification of a novel, large group of species-preserved cortical landmarks, but also new insights into the relationship between cortical folding patterns and axonal wiring diagrams along the evolution line.

**Keywords:** 3-hinge gyri · Structural connections · Comparative study

## 1 Introduction

Comparative neuroscience and neurology of primate brains have been of an intriguing research topic for decades in that they help to uncover the mechanism mediating the development and evolution of brains [1, 2]. They also provide insight into the nature of both inter-species commonalities for brain regions of basic function and the divergence of brain organization in charge of higher function. Such knowledge provides valuable clues to build animal models to many human neuroscience studies. To this end, effective approaches are needed to facilitate neuroanatomy comparison cross species [3]. However, because the morphology of both the anatomy and axonal pathway are hugely different across species, conventional image registration methods could not apply to cross-species alignment [3, 4]. Therefore, the comparative studies in the literatures either were limited by studying only a few cortical regions and white matter fasciculi, such as those related to vision [4] and language [1], or connectome that is based on brain parcellation scheme shared by species, such as Brodmann areas [5]. In

this respect, identification of a large group of species-preserved anatomical or connective landmarks could be an alternative approach to promoting cross-species comparative studies to a higher level.

Recently, a novel cortical convolution pattern, termed gyral hinge (white dots in Fig. 1(b)), the conjunction of several gyri, was found which possesses unique anatomical and connective profiles [6] in contrast to other cortical patterns. More importantly, correspondences of such gyral hinges were successfully found across human brains with huge variations and even across species. Moreover, corresponding gyral hinges were found to possess consistent white matter fiber morphologies across subjects and species [7]. Along this line, in this paper, we aim to investigate whether these gyral hinges can be used as landmarks for cross-species brain alignment. Using T1-weighted MRI and diffusion MRI (dMRI), we firstly adopted the method in [8] to identify gyral hinges of 3 spokes (3-hinge for short) on the entire cortices of human and macaque individuals. They were then used as nodes to infer dMRI derived individual connective matrix. Finally, a framework was proposed to establish correspondences of these 3-hinges across individuals and species by group-wisely matching the connective matrices. The results demonstrate that the identified corresponding 3-hinges possess consistent connective patterns across subjects and species, and the consistency outperforms those results obtained by conventional image registration methods. The cross-species correspondences were further validated by previous reports. Taken together, it proves promising to use them as landmarks for cross-species alignment, and also suggesting a new relationship between cortical folding and structural connection in species comparative studies.

## 2 Materials and Methods

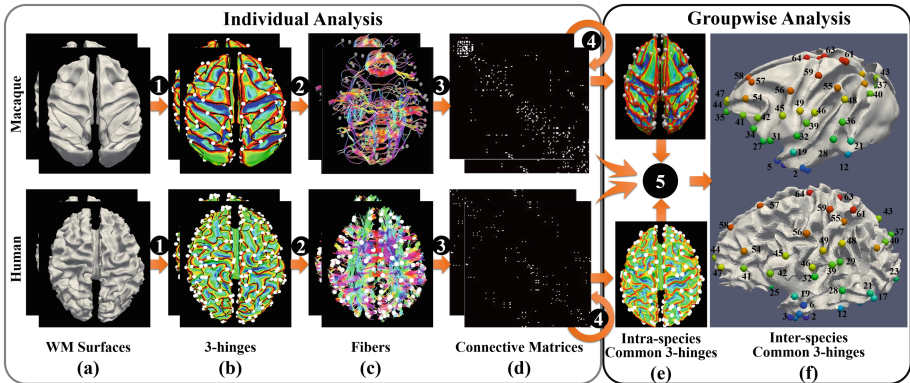
### 2.1 Overview

Figure 1 illustrates an overview of the analysis framework. In general, the aim of the work is to identify species-preserved 3-hinges in terms of their structural connectivities. The framework was divided to two parts. In the first part (shallow shade in Fig. 1), data processing and analysis were performed on individual space. White matter surfaces were reconstructed from T1-weighted MRI, on which 3-hinges are detected. dMRI derived deterministic streamline fibers were extracted if they connect any two of the 3-hinges, based on which individual connective matrix was constructed. In the second part (dark shade in Fig. 1), 3-hinges were identified which are consistent across subjects within species in terms of their connective patterns. Based on such group-wisely consistent 3-hinges and their connective matrices, the 3-hinges preserved across species were identified if the connective patterns of them are similar between the species.

### 2.2 Data Set Description and Pre-processing

**Human Brain Imaging:** The T1-weighted MRI and dMRI from the Q1 release of WU-Minn Human Connectome Project (HCP) consortium (<http://www.humanconnectome.org/>) were used in this study. Important imaging parameters are as follows: T1-weighted

MRI: voxel resolution  $0.7 \times 0.7 \times 0.7$  mm, TR = 2400 ms, TE = 2.14 ms, flip angle =  $8^\circ$ , image matrix =  $260 \times 311 \times 260$ . DMRI data: spin-echo EPI sequence; TR = 5520 ms; TE = 89.5 ms; flip angle =  $78^\circ$ ; refocusing flip angle =  $160^\circ$ ; FOV =  $210 \times 180$ ; matrix =  $168 \times 144$ ; spatial resolution =  $1.25 \text{ mm} \times 1.25 \text{ mm} \times 1.25$  mm; echo spacing = 0.78 ms. Each gradient table of the dMRI data includes approximately 90 diffusion weighting directions plus 6  $b = 0$  acquisitions. DMRI data consists of 3 shells of  $b = 1000, 2000, \text{ and } 3000 \text{ s/mm}^2$  with an approximately equal number of acquisitions on each shell within each run. Eighteen randomly selected subjects were used in this study.



**Fig. 1.** The framework of data processing and analysis. (a)–(d): the data processing steps 1–3 were in individual space and within species. (a) White matter cortical surfaces; (b) white dots represent the locations of 3-hinges and black curves represent gyral crest lines. Surfaces are color-coded by curvatures. Red regions have positive curvatures while blue ones have negative values; (c) streamline fibers that connect 3-hinges; (d) the structural connective matrices. Step 1: 3-hinge identification; step 2: extracting streamline fibers connecting the 3-hinges; step 3: reconstructing individual structural connective matrices based on (c). (e)–(f) intra-species and inter-species group-wise analyses. (e) Identified 3-hinges consistent across subjects within species *via* step 4; (f) Identified 3-hinges that have cross species correspondence *via* step 5.

**Macaque Brain Imaging:** UNC-Wisconsin neurodevelopment rhesus MRI database (T1 weighted MRI and dMRI data) was used in this work ([http://www.nitrc.org/projects/uncuw\\_macdevmri/](http://www.nitrc.org/projects/uncuw_macdevmri/)). 18 different subjects at the age of more than 12 months old were used. The resolution of T1-weighted MRI is  $0.27 \times 0.27 \times 0.27 \text{ mm}^3$  and a matrix of  $300 \times 350 \times 250$ . The basic parameters for diffusion data acquisition were: resolution of  $0.65 \times 0.65 \times 1.3 \text{ mm}^3$ , a matrix of  $256 \times 256 \times 58$ , diffusion-weighting gradients applied in 120 directions and  $b$  value of  $1000 \text{ s/mm}^2$ , as well as ten images with  $b = 0 \text{ s/mm}^2$ .

**Preprocessing:** Human data and macaque data share similar pipelines. T1-weighted MRI data was nonlinearly warped to FA map of dMRI data *via* FSL-fnirt [9]. White matter cortical surfaces were reconstructed from the registered T1-weighted MRI *via*

Freesurfer (<https://surfer.nmr.mgh.harvard.edu/>). For dMRI data, skull-strip and eddy currents were applied firstly, and then the model-free generalized Q-sampling imaging (GQI) method in DSI Studio [10] was used to estimate the density of diffusing water at different orientations. Deterministic fiber tracking algorithm [11] in DSI Studio was used to reconstruct  $4 \times 10^4$  fiber tracts for each subject using the default parameters.

### 2.3 Identification of 3-hinges and Reconstruction of Connective Matrix

We adopted the method in [8] to automatically identify the locations of 3-hinges on the entire white matter cortical surfaces ((a), (b) and step 1 in Fig. 1). In brief, the pipeline includes three steps: (1) Given the gyral altitudes (defined in [12]) for each vertex, the white matter cortical surface was segmented into gyral crests (regions over a predefined altitude level) and sulcal basins (regions below the level) *via* the watershed algorithm [13]; (2) A tree marching algorithm was used to construct a tree structure on gyral crests. The roots of the tree are located at the gyral crest centers that have the maximum distance values from crest borders, and all the other gyral crest vertices were recursively connected to them as branches and leaves till the crest borders were reached, following the descending gradients of the distance to the border; (3) We pruned the redundant branches if the path length is shorter than the predefined length threshold to preserve the main trunks as a gyral crest line network (black curves in Fig. 1(b)). The conjunction of the network, the connecting degrees of which are more than 3, are defined as gyral hinges. 3-hinges are of major interest in this work, as 4-hinges are very rarely seen.

To reconstruct structural connective matrix for 3-hinges, dMRI derived streamline fibers were extracted if they pass the neighborhoods (spheres centered at the locations of 3-hinges) of any two of the 3-hinges. The radius of the spheres is 2 mm for macaque and 4 mm for human with regard to their scales. Based on the extracted fibers, a connective matrix was constructed (Fig. 1(c) and (d), step 3 and 4), the nodes of which are the 3-hinges and the connective strength is the number of fibers connecting two 3-hinges.

### 2.4 Identification of Consistent 3-hinge Within Species

In Sect. 2.3, 3-hinge connective matrix was reconstructed on each individual. The numbers and locations of 3-hinges vary on different subjects and have no correspondence. Therefore, we established the correspondence of them within each species, by making the connective matrices consistent across subjects ((d), (e) and step 4 in Fig. 1).

Firstly, surfaces of all subjects were warped to the same spherical space *via* the spherical registration method in Freesurfer, to provide an anatomical constraint for the algorithm that will be detailed later. Then, we randomly selected a subject as a template which has  $n$  3-hinges, and its 3-hinge matrix is denoted by  $N$ . A global search was performed on the other subjects as testing subjects, respectively. For each of the template's 3-hinge, the 3-hinges on one testing subject (with  $m$  3-hinges and its 3-hinge matrix is denoted by  $M$ ) are in its search scope, or anatomical constraint, when they are within the geodesic distance of  $r$  mm. Altogether, the testing subject has  $n$  groups of candidate 3-hinges. Next, one candidate 3-hinge was selected from each search scope,

respectively. No overlap was allowed for the  $n$  candidates, and a connective matrix was constructed from them. This is equivalent to extracting an  $n \times n$  matrix  $N'$  from the original  $m \times m$   $M$  matrix. The matrix similarity was defined as  $\|N - N'\|_2$ . Because of the diagonal symmetry of  $N$  and  $N'$ , only the upper triangular part of them were used. Based on these steps, a similarity value was obtained for each selection of  $n$  candidates. The combinations of  $n$  candidates with the smallest similarity value gives the identified  $n$  3-hinges out of  $m$  original ones on the testing subject that correspond to the  $n$  3-hinges on the template. This algorithm was repeated on all testing subjects, and the final similarity values of all testing subjects were summed up as the score  $s$  for this template. It is noted that as  $N'$  and  $N$  should be of the same size, their dimension was determined by the subject who has the smallest 3-hinge number,  $n_s$ . Therefore, when this subject was selected as template, the above steps were performed only once. If another subject was selected as template,  $n_s$  out of  $n$  3-hinges were repeatedly selected to give the template  $n_s \times n_s$  matrix. The smallest similarity value between the selection on the template and the selection on the testing subject was considered as the optimal result. Finally, the template with the smallest score  $s$  together with the identified corresponding  $n_s$  3-hinges on all other subjects were obtained. As the computation load was largely determined by repeatedly selecting a  $n_s \times n_s$  matrix on either a  $n \times n$  template matrix or a  $m \times m$  testing subject matrix ( $310 \pm 5$  3-hinges for human and  $130 \pm 2$  for macaque), the simulated annealing algorithm was adopted to reduce the computation load [14].

## 2.5 Identification of Species-Preserved 3-hinge

In Sect. 2.4, we obtained  $n_s^m$  corresponding 3-hinges for all macaques and  $n_s^h$  3-hinges for all humans. We established the correspondence between the two groups of 3-hinges *via* the similar global search method. Because the template for each species was identified and all subjects within each species are in the same space, warping the human template to the macaque template ensures all subjects are roughly in the same space. Macaque was used as the cross-species template because  $n_s^m < n_s^h$ . The search scope for macaque 3-hinges on human brains was computed in a group-wise manner. The corresponding  $i^{th}$  3-hinges from all the macaque subjects were used to determine their centroid in the common space, and the geodesic radius  $r$  was used with the centroid to give the search scope. For each human subject, the 3-hinges fall in this search scope were selected as candidates, such that each human individual had a candidate set. Only those in the intersection of all individual candidate sets were considered as the effective candidates for the  $i^{th}$  3-hinge on macaque, because the locations of corresponding 3-hinges on different human subjects are varied even in the common space. To conduct the global search, a combination of  $n_s^m$  candidates were selected to give 18 individual connective matrices for human. Pairwise matrix similarities between these 18 human matrices and 18 macaque matrices were computed and the mean similarity value was defined as the group-wise cross-species similarity for this candidate combination. Likewise, simulated annealing algorithm was adopted to identify the optimal  $n_s^m$  candidates on human with the minimal similarity value.

### 3 Results

#### 3.1 Identified Corresponding 3-hinges Within Species

The radius of search scope  $r$  is 2 mm for macaque intra-species search scope and 4 mm for human due to their size scales. 128 and 306 3-hinges with correspondence were respectively identified for macaque and human. Their locations, as well as the streamlines fibers connecting them and the connective matrices on four example subjects for each species, are shown in Fig. 2(a)–(c). The inter-individual consistency can be observed with regard to the similar fiber bundle morphologies and connective matrices.

Statistically, for each species, we measured the similarity of the 3-hinge connective matrices for each subject pair. The similarity was defined as the Pearson correlation coefficient of the upper triangular parts of two matrices. The results are shown in Fig. 2(d). On average, the inter-individual similarity (the diagonal lines in Fig. 2(d) were omitted) is  $0.55 \pm 0.11$  for macaque and  $0.14 \pm 0.09$  for human. These results were compared to those based on spherical registration method in Freesurfer, by which the 3-hinge correspondence was determined by search for the closest 3-hinge on a registered testing subject to that on the template. Spherical registration method was used for this comparison because of its good performance in cortical pattern alignment within and across species so far [3]. On average, the inter-individual similarity is  $0.31 \pm 0.16$  for macaque and  $0.09 \pm 0.10$  for human, which are much lower than those by our method.

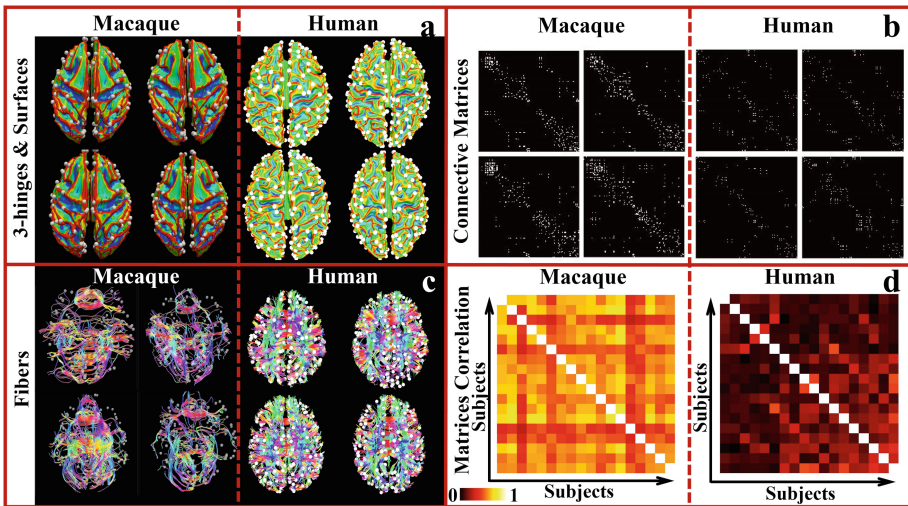


**Fig. 2.** Intra-species analysis results. (a)–(b) four subjects randomly selected for each species are used as examples; (a) identified 3-hinges with correspondence across subjects. Surfaces with curvature map are shown as background; (b) Connective matrices of the 3-hinges in (a). The matrices are binarized (connective strength of the white elements  $> 0$ ) for ease of visualization. (c) The streamline fibers connecting the 3-hinges in (a). (d) Similarity of connective matrices in (b) of all 18 subjects within each species.



### 3.2 Identified Species-Preserved 3-hinges

As macaque has 128 intra-species consistent 3-hinges, 128 inter-species corresponding 3-hinges were identified in the human brain. The correspondences are visualized in Fig. 3(a). Streamline fibers connecting these 3-hinges on example subjects of both species are in Fig. 3(b). The connective matrices average within species are shown in

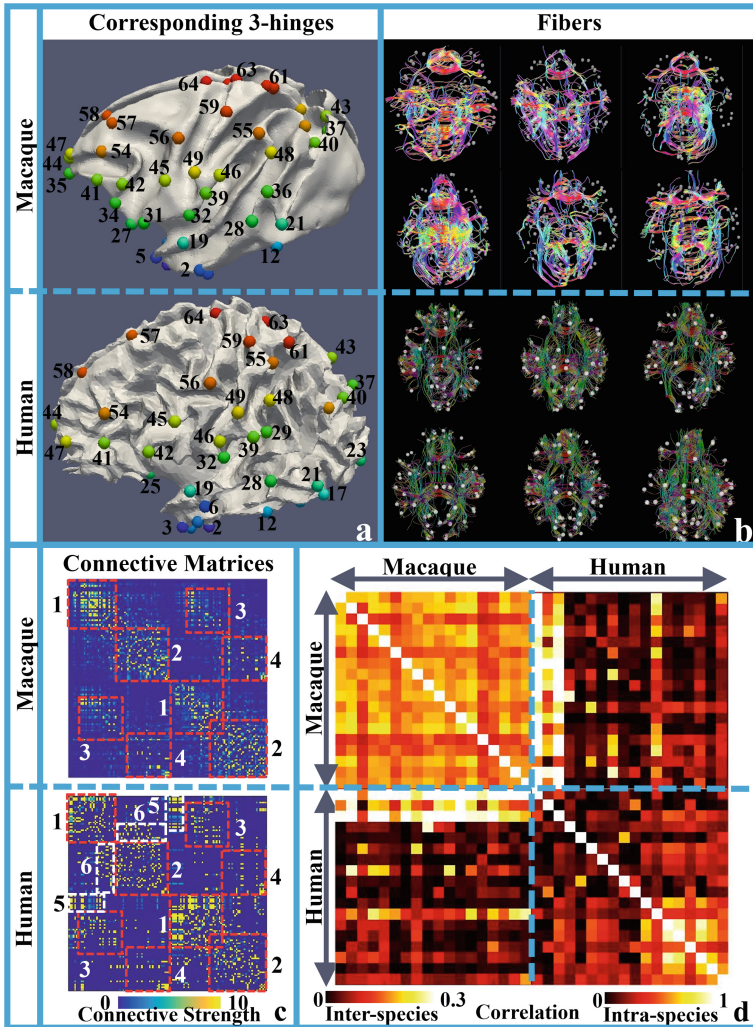


**Fig. 3.** (a) Species-preserved 3-hinges with the corresponding IDs; (b) streamline fibers connecting the 3-hinges in (a) on example subjects; (c) the structural connective matrix averaged over subjects within species. Red boxes highlighted the similarity between two species while white boxes highlight the differences; (d) the inter-individual and cross-species similarity of connective matrices of these 3-hinges in (a). For the ease of visualization, diagonal blocks (intra-species similarity) and off-diagonal-line blocks (inter-species similarity) are at different color scales.

Fig. 3(c) as well. The cross-species similarity is observable with regard to the fiber bundle morphologies in Fig. 3(b) and connective pattern highlighted by red boxes in Fig. 3(c). The inter-individual and inter-species similarity of the connective matrices are shown in Fig. 3(d). On average, the inter-species similarity, averaged over the off-diagonal-line block, is  $0.08 \pm 0.06$ , and the intra-species similarity for human is  $0.23 \pm 0.20$ . The intra-species similarity for macaque is the same as the one in Sect. 3.1. These results outperform those based on spherical registration method:  $0.05 \pm 0.09$  for the inter-species similarity and  $0.09 \pm 0.12$  for the intra-species on human brains.

The identified species-preserved 3-hinges and connective fibers are in line with previous reports [1, 2]. For example, the red boxes highlighted species-preserved blocks #1 and #3 that are the ipsilateral and contralateral connections within temporal lobe and occipital lobe. Blocks #2 and #4 are the ipsilateral and contralateral connections within frontal lobe and parietal lobe. Blocks #5 highlight the connections between temporal lobe and the contralateral temporal pole. Blocks #6 highlight the ipsilateral connections between temporal lobe and inferior frontal lobe/parietal lobe. Blocks #5 and #6 are unique for humans.

## 4 Conclusion

We present a framework to establish cross-species correspondence for cortical 3-hinges in terms of their structural connective patterns, which is in line with previous reports, suggesting that they can be used as landmarks for cross-species alignment. This work could reveal the relation between cortical convolution and structural connection across species, shedding new light to comparative neuroscience studies of primate species.

**Acknowledgements.** T Zhang was supported by NSFC31671005 and NSFC31500798.

## References

1. Rilling, J.K., et al.: The evolution of the arcuate fasciculus revealed with comparative DTI. *Nat. Neurosci.* **11**(4), 426–428 (2008)
2. de Schotten, M.T., Dell’Acqua, F., Valabregue, R., Catani, M.: Monkey to human comparative anatomy of the frontal lobe association tracts. *Cortex* **48**(1), 82–96 (2012)
3. Van Essen, D.C.: Surface-based approaches to spatial localization and registration in primate cerebral cortex. *Neuroimage* **23**, S97–S107 (2004)
4. Orban, G.A., Van Essen, D., Vanduffel, W.: Comparative mapping of higher visual areas in monkeys and humans. *Trends Cogn. Sci.* **8**(7), 315–324 (2004)
5. Van Essen, D.C., Dierker, D.L.: Surface-based and probabilistic atlases of primate cerebral cortex. *Neuron* **56**(2), 209–225 (2007)
6. Li, K., et al.: Gyral folding pattern analysis via surface profiling. *NeuroImage* **52**(4), 1202–1214 (2010)
7. Li, X., et al.: Commonly preserved and species-specific gyral folding patterns across primate brains. *Brain Struct. Funct.* **222**(5), 2127–2141 (2017)



8. Chen, H., Li, Y., Ge, F., Li, G., Shen, D., Liu, T.: Gyral net: a new representation of cortical folding organization. *Med. Image Anal.* **42**, 14–25 (2017)
9. Andersson, J.L.R., Jenkinson, M., Smith, S.L.: Non-linear registration, aka spatial normalisation. FMRIB Technical report TR07JA2 (2010)
10. Yeh, F.C., Wedeen, V.J., Tseng, W.Y.I.: Generalized q-sampling imaging. *IEEE Trans. Med. Imaging* **29**(9), 1626–1635 (2010)
11. Yeh, F.C., Verstynen, T.D., Wang, Y., Fernández-Miranda, J.C., Tseng, W.Y.I.: Deterministic diffusion fiber tracking improved by quantitative anisotropy. *PLoS ONE* **8**(11), e80713 (2013)
12. Fischl, B., Sereno, M.I., Tootell, R.B., Dale, A.M.: High-resolution intersubject averaging and a coordinate system for the cortical surface. *Hum. Brain Mapp.* **8**(4), 272–284 (1999)
13. Bertrand, G.: On topological watersheds. *J. Math. Imaging Vis.* **22**(2–3), 217–230 (2005)
14. Granville, V., Krivánek, M., Rasson, J.P.: Simulated annealing: a proof of convergence. *IEEE Trans. Pattern Anal. Mach. Intell.* **16**(6), 652–656 (1994)